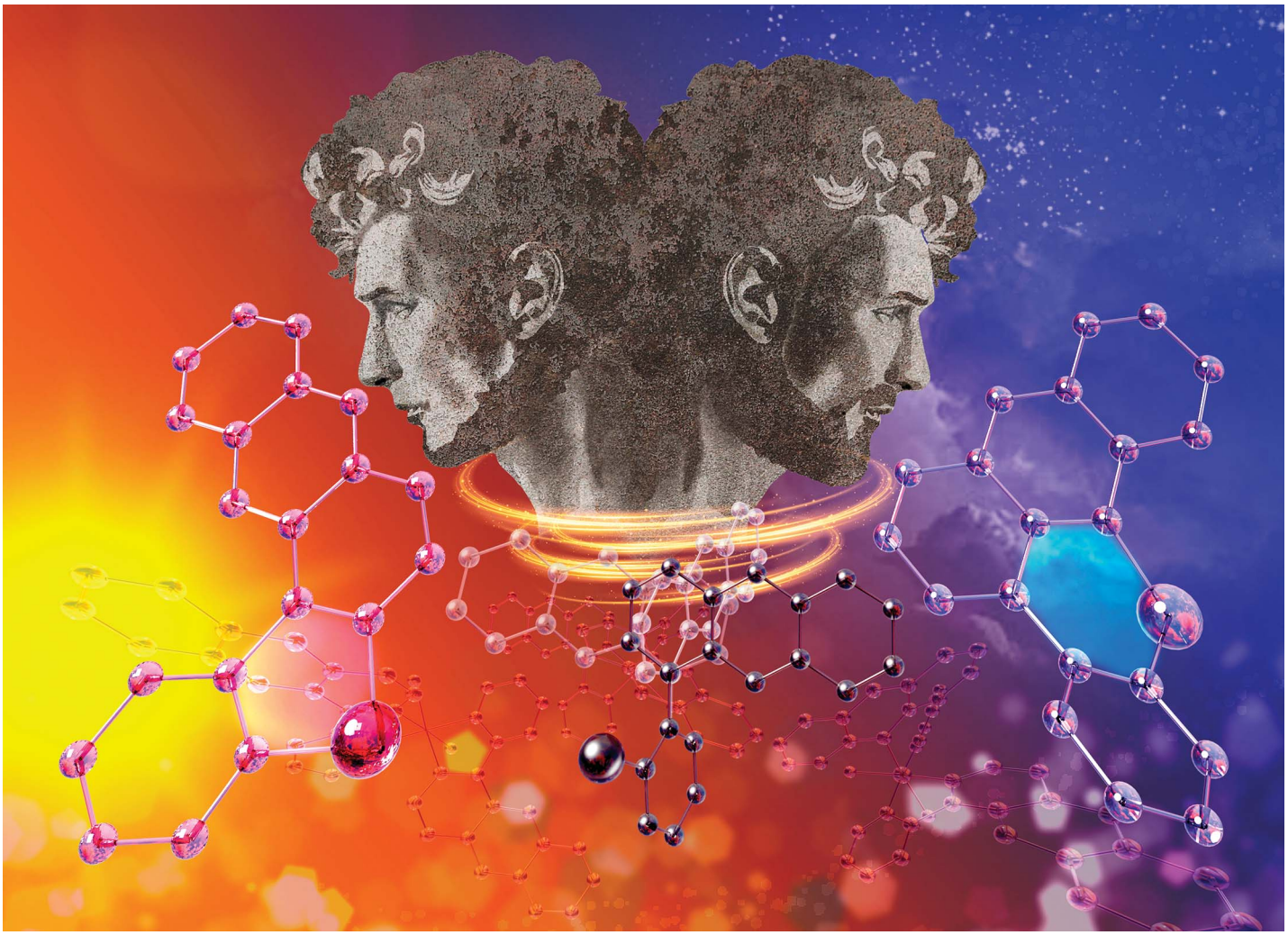

Showcasing research from Professor Mark MacLachlan's Laboratory, Department of Chemistry, The University of British Columbia, Vancouver, Canada.

π-Extended ligands with dual-binding behavior: hindered rotation unlocks unexpected reactivity in cyclometalated Pt complexes

This cover image, designed by Japanese graphic designer Satohiro Tatara (TATARAS Design), illustrates the dual binding behavior of Pt complexes featuring π-extended ligands with two faces, reflecting the dual faces of the Roman god Janus. The structures also depict the slow rotation of a free aryl ring, which facilitates the formation of both 5-membered and 6-membered rings. The red and blue colors emphasize the difference in ring sizes.

As featured in:

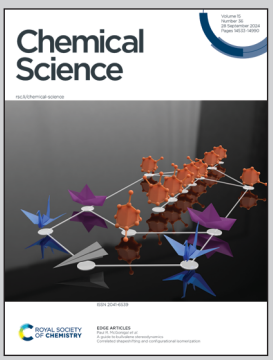

See Miguel A. Soto, Mark J. MacLachlan *et al.*, *Chem. Sci.*, 2024, **15**, 14644.

ROYAL SOCIETY OF CHEMISTRY

rsc.li/chemical-science

Registered charity number: 207890

Chemical Science

ROYAL SOCIETY OF CHEMISTRY

EDGE ARTICLE

View Article Online
View Journal | View Issue

Cite this: *Chem. Sci.*, 2024, **15**, 14644

All publication charges for this article have been paid for by the Royal Society of Chemistry

π-Extended ligands with dual-binding behavior: hindered rotation unlocks unexpected reactivity in cyclometalated Pt complexes†

Seiya Ota, [a] Miguel A. Soto, *[a] Brian O. Patrick, [a] Saeid Kamal, [a] Francesco Lelj [b] and Mark J. MacLachlan *[acd]

Cyclometalated platinum complexes play a crucial role in catalysis, bioimaging, and optoelectronics. Phenylpyridines are widespread cyclometalating ligands that generate stable and highly emissive Pt complexes. While it is common practice to modify these ligands to fine-tune their photophysical properties, the incorporation of polycyclic aromatic hydrocarbons into the ligand's structure has been largely overlooked. This report describes the cyclometalation of naphthalenyl- and anthracenylpyridine ligands, which has resulted in ten new luminescent Pt^{II} and Pt^{IV} complexes. These species are enabled by a dual-binding behavior discovered in our polyaromatic-containing ligands. The introduction of naphthalenyl and anthracenyl groups unlocks dual binding modes, with the Pt center bonding to either of two distant carbon atoms within the ligand. These complexes exhibit both symmetric structures with two 5-membered metallacycles and asymmetric structures with 5- and 6-membered metallacycles. This work presents a strategy for the regioselective synthesis of Pt complexes with bespoke structures and photophysical properties. Our findings offer new opportunities in platinum chemistry and beyond, with potential implications for materials and technologies.

Received 18th July 2024
Accepted 22nd August 2024

DOI: 10.1039/d4sc04799k

rsc.li/chemical-science

Introduction

Cyclometalated platinum complexes have been the subject of extensive research in the last few decades due to their unique photophysical properties, reactivity, and stability.[1–4] Many cyclometalating ligands have been reported in the literature, with arylpyridines[5–7] and bis(aryl)pyridines[7,8] being among the most studied. These structurally tailorable ligands are easy to access and once bound to Pt impart unique properties for various applications, including bioimaging,[9–11] optoelectronics,[12,13] sensing,[14,15] and catalysis.[16,17]

A number of cyclometalated Pt species reported to date rely on phenylpyridine-based ligands.[8,18–30] The simplest examples of this family consist of 2-phenylpyridine and Pt^{II} or Pt^{IV} centers (Fig. 1a). Several research groups have tailored these systems in different directions to fine-tune the photophysical properties of the resulting complexes.[31–33] Our group has been particularly inspired by these and other examples to incorporate phenylpyridine-based complexes in supramolecular assemblies,[34] focusing primarily on (i) bridging phenylpyridines with a single oxygen atom,[35] (ii) appending ring molecules to

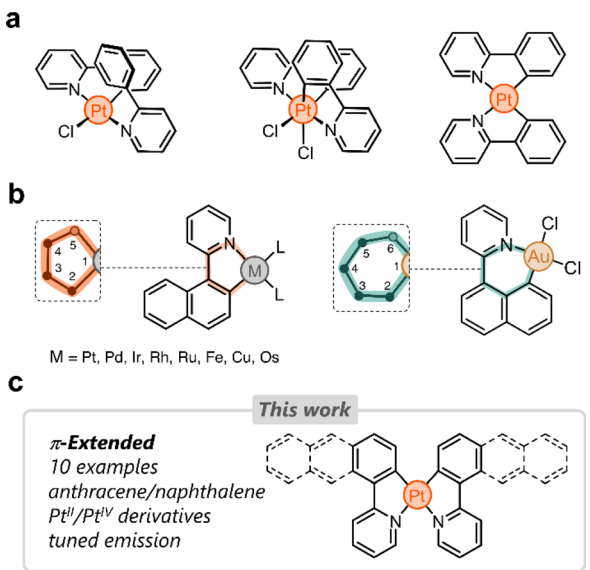

Fig. 1 (a) Selected examples of cyclometalated Pt^{II} and Pt^{IV} complexes based on 2-phenylpyridine. (b) Dual binding behavior of 2-(naphthalen-1-yl)pyridine with various metals. (c) This work's overview.

[a]Department of Chemistry University of British Columbia, 2036 Main Mall, Vancouver, V6T 1Z1, Canada. E-mail: msoto@chem.ubc.ca; mmaclach@chem.ubc.ca
[b]La.M.I.and LaSCAMM INSTM Sezione Basilicata, Dipartiento di Scienze, Università della Basilicata, via dell'Ateneo Lucano 10, Potenza, 85100, Italy
[c]Stewart Blusson Quantum Matter Institute University of British Columbia, 2355 East Mall, Vancouver, BC, V6T 1Z4, Canada
[d]WPI Nano Life Science Institute Kanazawa University, Kanazawa, 920-1192, Japan

† Electronic supplementary information (ESI) available. CCDC 2357023–2357030. For ESI and crystallographic data in CIF or other electronic format see DOI: https://doi.org/10.1039/d4sc04799k

phenylpyridines,[36,37] and (iii) incorporating flexible linkers to shape Pt-bridged macrocycles.[38]

Despite the growing interest in phenylpyridine ligands, studies on derivatives containing π-extended polyaromatics are scarce. Specifically, only 2-(naphthalen-1-yl)pyridine has been investigated in the cyclometalation of Pt,[39] Pd,[40] Ir,[41] Rh,[42] Ru,[43] Fe,[44] Cu,[45] and Os.[46] In these examples, the ligand binds to the metal *via* the pyridine's nitrogen donor and through a carbon atom from the naphthalenyl group (2-position, C2). This results in the formation of 5-membered metallacycles (Fig. 1b).[47] When the same ligand forms a complex with Au, the naphthalenyl unit binds to the metal through the carbon at position 8 (C8), yielding a 6-membered metallacycle (Fig. 1b). This regioselective behavior has been observed only in heteroleptic Au complexes to date.[48] We hypothesized that the dual binding behavior that the naphthalenyl motif displays could be exploited in other polyaromatics appended to a pyridine donor. This could uncover new directions in chemical reactivity as well as enable tailoring of the emission in the resulting Pt complexes.

Here we investigate the cyclometalation of phenyl-, naphthalenyl-, and anthracenylpyridine ligands (Fig. 1c). By exploiting the dual binding behavior of naphthalenyl and anthracenyl groups, we have isolated ten new cyclometalated complexes, with Pt^{II} and Pt^{IV} centers. These display tunable photoluminescence from blue to infrared light. All complexes have been characterized and analyzed through 1-D and 2-D nuclear magnetic resonance (NMR) spectroscopy, UV-vis spectroscopy, fluorescence spectroscopy, high-resolution mass spectrometry (HRMS), density-functional theory (DFT), and single-crystal X-ray diffraction (SCXRD).

Results and discussion

The three target ligands are shown in Scheme 1a–c. Compound **1** (2-phenylpyridine) was purchased and used without purification. Ligand 2-(naphthalen-1-yl)pyridine (**2**) was synthesized through the Suzuki cross-coupling of naphthalen-1-ylboronic acid and 2-bromopyridine (91% yield).[49] 2-(Anthracen-1-yl) pyridine (**3**) was obtained in three steps. First, 1-aminoanthracene-9,10-dione was converted to 1-bromoanthracene *via* a Sandmeyer reaction, followed by reduction.[50] The product was borylated *via* a Miyaura borylation,[51] and then coupled with 2-bromopyridine to obtain ligand **3** in 35% overall yield (full details in ESI†).

In the direct metalation of 2-phenylpyridine, the ligand (**1**) is typically reacted with $K_2[PtCl_4]$ in polar media, leading to the formation of the Pt^{II} square planar complex **1a** (Scheme 1a).[20] This compound has one cyclometalated phenylpyridine (forming a 5-membered metallacycle) and another one only *N*-coordinated, with a free phenyl ring. The coordination sphere of the metal center is completed by a Cl^- ion. With this in mind, we tested the direct metalation of ligands **2** and **3**, anticipating that their reactivity would be similar to **1**.

After metalation, complexes **2a** and **3a** (Scheme 1b and c) were isolated and their structures were unequivocally assigned by SCXRD. Both molecules have one cyclometalated ligand and another one coordinated only through the pyridine unit (Fig. 2a). Crystals of **2a** have two molecules in the asymmetric unit, both with the cyclometalated and free naphthalenyl groups facing opposite directions. Similarly, **3a** has two molecules in the asymmetric unit, one that has a similar geometry to **2a** and a second one with the free and cyclometalated anthracenyl groups facing in the same direction, with an interplanar distance averaging 5.75 Å and a 48° deviation from coplanarity (see Fig. 2b).

Complexes **2a** and **3a** were characterized in solution using ^1H NMR spectroscopy; the recorded spectra were more intriguing than expected (full data in Fig. S1†). For comparison, complex **1a** displays distinct signals for each of its phenylpyridine units,[20] with resonances attributed to protons *a* and *a′* at 9.6 and 9.2 ppm (Fig. 2c), respectively. However, for **2a** and **3a**, each of these resonances split into two signals (*e.g.*, d = 9.6, 9.3, 9.23 and 9.17 ppm for **2a**, Fig. 2c). Exchange spectroscopy (EXSY) NMR of **2a** and **3a** confirmed that the two sets of protons undergo exchange at room temperature (Fig. 2d and S2†). This suggested that in solution two atropisomers may interconvert through slow rotation of the unbound aryl units (naphthalenyl and anthracenyl) in **2a** and **3a**.

The initial support for this hypothesis comes from the solid-state structure of **3a**, which revealed two distinct atropisomers in the crystal lattice (Fig. S3†). Subsequent investigation using variable-temperature ^1H NMR spectroscopy showed that the exchanging resonances for both **2a** and **3a** broaden as the temperature exceeds 90 °C (see Fig. S4 and S5†). DFT analysis showed that the interconversion is likely due to slow rotation about the C–C bond that connects the unbound aryl groups with the pyridine unit (Fig. 2e and ESI†). The computed activation barriers are 19.2 and 20.4 kcal mol^{-1} for **2a** and **3a**, respectively. These values are in good agreement with those obtained experimentally by ^1H–^1H EXSY NMR spectroscopy, which correspond to 18.4 (**2a**) and 19.1 kcal mol^{-1} (**3a**) in DCM-d_2 at 25 °C (Fig. S6 and Table S1†). In contrast, the rotation along the same C–C bond in **1a** (containing a phenyl ring) occurs with a much lower energy barrier (7.7 kcal mol^{-1}, see ESI†) – this explains the observation of only one species by ^1H NMR spectroscopy. It is noteworthy that the rotation about the N–Pt bond may have a negligible effect on the exchange process due to its higher activation barrier, estimated to range from 26 to 33 kcal mol^{-1} in **1a**, **2a** and **3a** (see ESI, Fig. S7, S8 and Table S2†).

The unexpected slow interconversion of rotamers raised the question of whether this behavior would influence the reactivity of **2a** and **3a** towards oxidation (Scheme 1b and c). Typically, treating compound **1a** with $PhICl_2$ leads to oxidation of the metal center (Pt^{II} to Pt^{IV}) and cyclometalation of the free phenyl ring, generating compound **1b** (Scheme 1a).[22] A similar outcome was expected from **2a** and **3a**, and thus their oxidations were tested.

In a representative experiment, a solution of **2a** in DCM-d_2 was treated with 1 equiv of $PhICl_2$ at room temperature, and the resulting mixture was analyzed by ^1H NMR spectroscopy (Fig. S9†). Upon addition of the oxidant, all resonances corresponding to **2a** disappeared, confirming its conversion into a new species. Based on the precedent of converting **1a** to **1b**, it

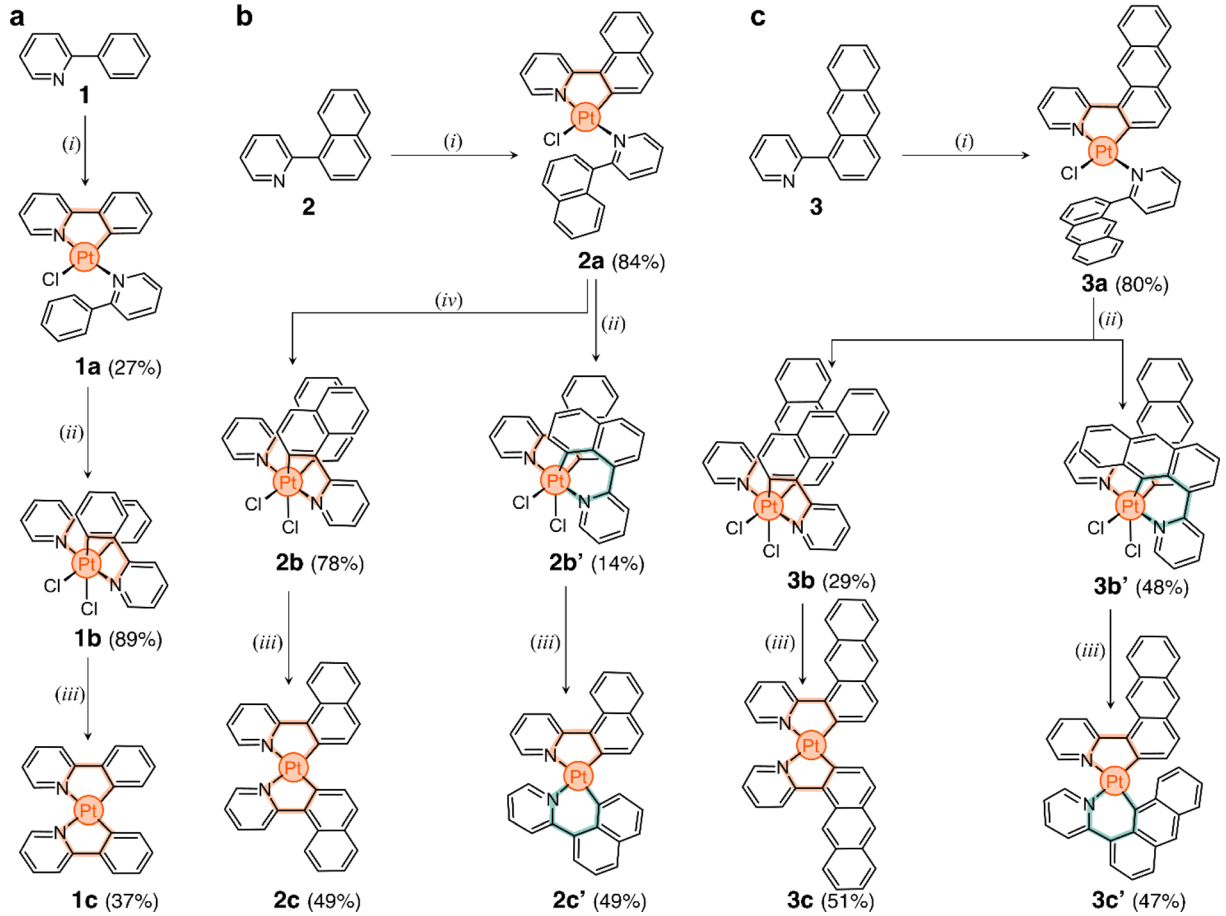

Scheme 1 Synthesis of cyclometalated Pt complexes using (a) phenyl-, (b) naphthalenyl-, and (c) anthracenylpyridine ligands **1**, **2**, and **3**. Reaction conditions: (i) $K_2[PtCl_4]$, H_2O, 2-ethoxyethanol, 80 °C, N_2; (ii) $PhICl_2$, DCM, 25 °C; (iii) *t*-BuOK, THF, 60 °C, N_2; (iv) $PhICl_2$, 1,1,2,2-tetrachloroethane, 130 °C.

was anticipated that the product would also have C_2 symmetry. However, the recorded ^{1}H NMR spectrum showed many resonances (Fig. 3a), suggesting the formation of more than one product. Taking advantage of subtle solubility differences between the products, a new compound, **2b′** (Scheme 1b), was first isolated in 14% yield. HRMS confirmed that **2b′** contains a Pt center and two deprotonated cyclometalating ligands ([**2b′** − Cl]$^+$, *m*/*z* (exp.) = 638.0953 Da, *m*/*z* (calc.) = 638.0963 Da). The ^{1}H NMR spectrum of **2b′** showed individual sets of resonances for each naphthalenylpyridine unit, with the α-pyridine protons *a* and *a′* appearing at 10.2 and 10.0 ppm (Fig. 3a). The solid-state structure (SCXRD) of **2b′** proved that each ligand binds to Pt with a distinct coordination mode. As shown in Fig. 3c, one of the ligands coordinates to the Pt center *via* the C2 naphthalenyl carbon atom, forming a 5-membered metallacycle. The second ligand cyclometalates to Pt generating a 6-membered ring *via* C8-ligation to the naphthalenyl group.

We were unable to isolate the anticipated product **2b** (Scheme 1b) in sufficient purity. DFT calculations performed on both **2b** and **2b′** revealed that **2b** is thermodynamically more stable than **2b′** by 3–4 kcal mol^{-1} (see ESI, Table S3 and S4†). Considering this, **2a** was treated with $PhICl_2$ in 1,1,2,2-tetrachloroethane at 130 °C. A ^{1}H NMR spectrum of the isolated product showed only one set of signals (see, *e.g.*, proton *a* at 10.1 ppm, Fig. 3a), indicating the selective formation of **2b**. This compound (78% yield) was analyzed by SCXRD (Fig. 3b), confirming that it contains a Pt^{IV} center coordinated to two Cl$^-$ ions and two cyclometalating ligands. Similar to **1b**,[22] **2b** also contains two ligands forming 5-membered metallacycles (C2-ligated).

Oxidation of the anthracene-based compound **3a** was also tested, resulting in the detection of two products in a 1 : 2 ratio in the crude reaction product (Fig. S10†). Compounds **3b** and **3b′** (Scheme 1c) were obtained in 29% and 48% yield, respectively, after purification. Notably, we were able to purify **3b** and **3b′** by silica gel column chromatography, in contrast to the more challenging purification of **2b** and **2b′**. SCXRD analysis confirmed that the two complexes have analogous structures to **2b** and **2b′** (see Fig. 3b and c). Compound **3b′** has 5- and 6-membered metallacycles, with the Pt^{IV} center bound to the C2 and C9 carbon atoms of the anthracenyl units, respectively, while **3b** has two 5-membered metallacycles (C2-bound).

We envisioned that the unexpected reactivity of **2a** and **3a**, enabled by the dual-binding behavior of anthracenyl and naphthalenyl groups, would serve as a unique handle to trap other unpredicted cyclometalated species, especially in the

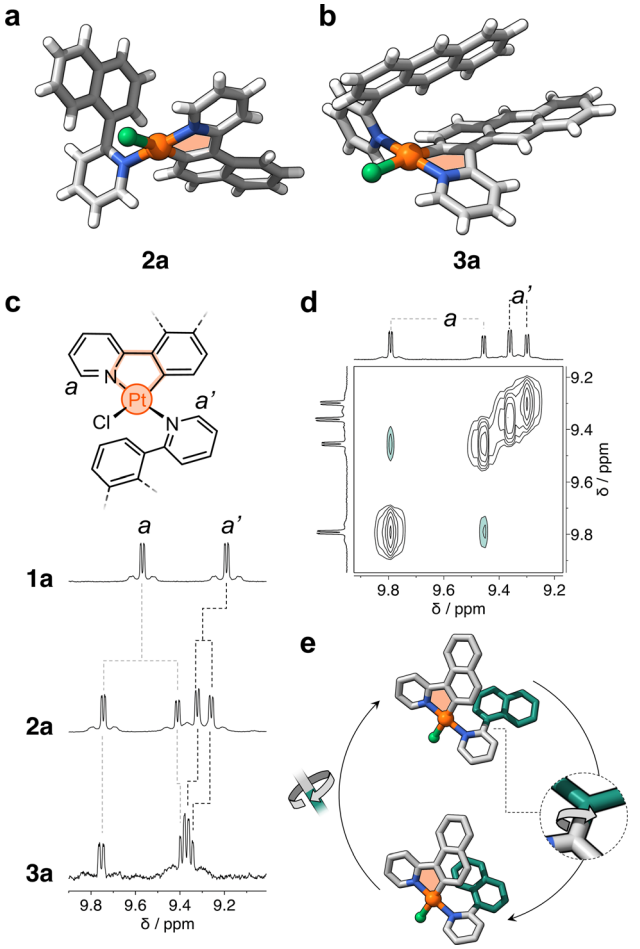

Fig. 2 Solid-state molecular structures of complexes (a) **2a** and (b) **3a**. (c) Representative chemical structure of complexes **1a**, **2a**, and **3a**. Partial ^{1}H NMR spectra (400 MHz, DCM-d_2) of such complexes is shown in this panel. (d) Partial EXSY NMR spectrum (600 MHz, DCM-d_2) of complex **2a** showing cross peaks between the signals of two atropisomers. (e) Proposed rotational dynamics observed in complex **2a** in solution. The structures correspond to the two DFT-computed isomers. Hydrogen atoms omitted for clarity. The cyclometalated and free-rotating naphthalenyl moieties are colored grey and green, respectively.

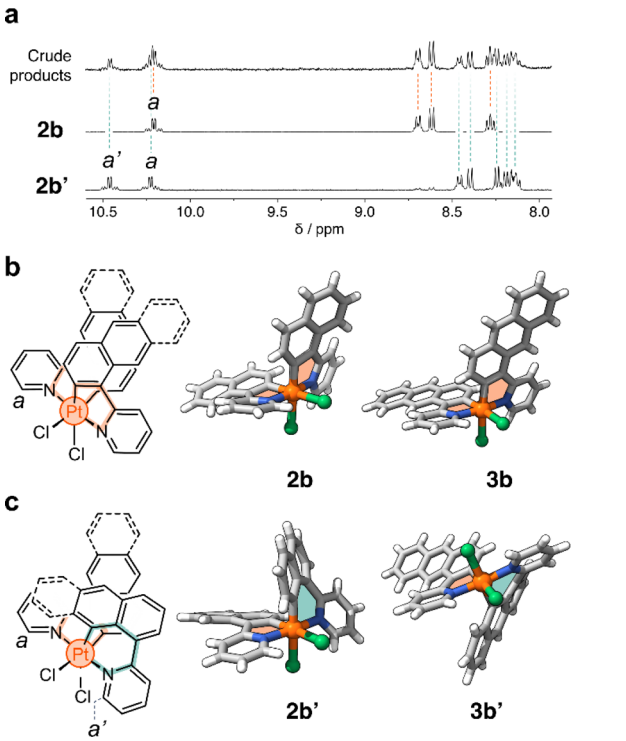

Fig. 3 (a) Partial ^{1}H NMR spectra (400 MHz, DCM-d_2) of the reaction crude product obtained from the oxidation of **2a**. (b) Chemical structure and solid-state structures of complexes (b) **2b** and **3b**, and (c) **2b′** and **3b′**. Panels (b) and (c) contain the proton assignment of resonances *a* and *a′*.

form of Pt^{II} complexes. For this, reduction of the four Pt^{IV} species **2b**, **2b′**, **3b**, and **3b′** was tested (Scheme 1b and c). All compounds were heated at 60 °C with 20 equiv of *t*-BuOK in THF under a N_2 atmosphere.[52] The reaction mixtures were purified using column chromatography and the expected products were isolated in yields of 47% to 51% (details in ESI†).

Fig. 4a shows the partial ^{1}H NMR spectra of compounds **2c** and **2c′** (full data in ESI†). In comparison to their precursors, **2b** and **2b′**, some of the resonances (*e.g.*, *a*) show an upfield shift ($\Delta\delta_a = -1.3$ ppm and -1.4 ppm, respectively), indicating the successful reduction of Pt^{IV} to the less electrophilic Pt^{II} center. The ^{1}H NMR spectrum of **2c′** contains twice the number of resonances as its analogue **2c**. This decreased symmetry is also observed in the ^{13}C{^{1}H} NMR spectrum, with thirty ^{13}C signals detected for **2c′** and only fifteen for **2c** (Fig. S11†). Similarly, the ^{1}H NMR spectrum of **3c′** showed twice as many resonances as that of its analogue **3c**, clearly indicating a significant reduction in symmetry. This observation suggests a more complex and less symmetrical environment in **3c′**, which is also confirmed by the 38 resonances observed in the ^{13}C{^{1}H} NMR spectrum of this complex compared to the 19 signals observed for compound **3c** (see Fig. S12†).

The molecular structures of complexes **2c** and **3c** were determined by SCXRD (Fig. 4b and c). Each molecule has two flat 5-membered metallacycles, although with noticeable deviation from the ideal square planar geometry of the Pt center. Specifically, the dihedral angles (θ) are 26° and 28° for **2c** and **3c**, respectively. This deviation, which has been observed in previous studies,[19] originates from steric repulsion between hydrogen atoms on the ligand (*e.g. a* in Fig. 4b and c). Unfortunately, attempts to obtain single crystals of **2c′** and **3c′** failed, so insights into their structures were gained through DFT computations (see ESI, Table S5†). Complexes **2c′** and **3c′** show minimal deviation from first coordination square planar geometry, with θ of 5° and 3°, respectively (Fig. 4d and e). This distortion is attributed to the boat-like conformation adopted by the six-membered metallacycles, where the aryl and pyridine rings deviate from the plane of the coordination sphere. This deviation effectively mitigates the steric repulsion between adjacent hydrogen atoms in complexes **2c** and **3c**.

After isolating ten different complexes from ligands **2** and **3**, we investigated their emission properties and compared them with those of **1a**, **1b**, and **1c**,[8,19,20] (Fig. S13 to S16†). All

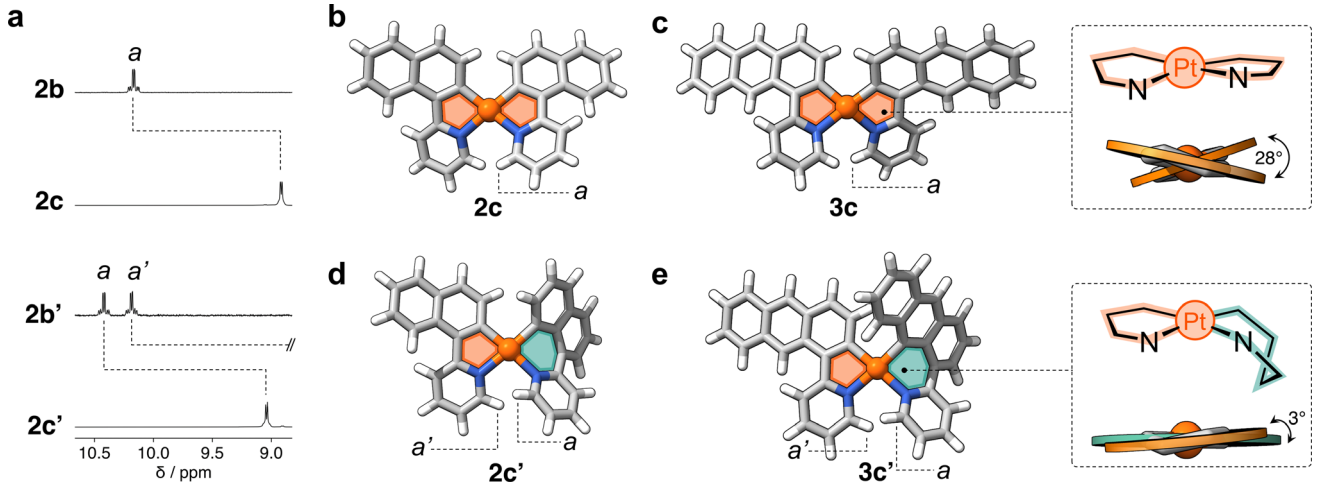

Fig. 4 (a) Partial ^{1}H NMR spectra (400 MHz, DCM-d_2) of complexes **2c** and **2c′** and their precursors **2b** and **2b′**. (b) Crystal structures as determined by SCXRD of complexes (b) **2c**, (c) **3c**, and DFT-minimized structures of (d) **2c′** and (e) **3c′**. Panels (c) and (e) depict the conformation of the 5- and 6-membered metallacycles as well as the dihedral angles in complexes **3c** and **3c′**.

complexes except for **1c** exhibited long emission lifetimes (up to 15 μs) in solution and relatively low photoluminescent quantum yields (Φ). Compound **2a** had the highest Φ (2.3%, Table S6†).

In addition, the collected data shed light on several important aspects. First, the compounds exhibit a concomitant redshift of their absorption and emission bands as the ligand's π-conjugation extends from phenyl (**1**) to naphthalenyl (**2**) to anthracenyl (**3**). For instance, in solution, compounds **1a**, **2a**, and **3a** emit green, orange, and red-to-infrared light, respectively (see Fig. 5a). Related complexes have been previously reported in the literature to undergo photoinduced isomerization.[30] However, the consistency of the UV-vis absorption and excitation spectra indicated that this is not the case for the compounds investigated here. It should be noted that the excitation spectra for some complexes were not recorded owing to their very weak emission (see Fig. S15†). The CIE plot in Fig. 5b illustrates the significant differences in emission that can be achieved within this family of compact emitters. Additionally, the sets of isomers, such as **2b**/**2b′** and **3b**/**3b′**, show similar photophysical properties. The emission bands of **2c** and **2c′** differ in a range of 10 to 42 nm in solution, in a glassy matrix, and in the solid state (Fig. S17†), indicating that subtle structural differences can fine-tune emission properties. Finally, for some complexes, luminescence is activated by switching from phenyl to naphthalenyl or anthracenyl. Although compound **1c** is not luminescent in solution, the analogous complexes formed with ligands **2** and **3** are emissive. This may be due to the significant deviation from planarity that **1c** (θ > 80°) shows in the excited state, which promotes non-radiative decay.[53,54] However, this phenomenon may be reduced in complexes **2c**, **2c′**, **3c**, and **3c′** with bulkier ligands. Altogether, these observations indicate potential areas for further exploration, such as customizing the emission properties of cyclometalated Pt complexes by expanding to other polyaromatics. In addition, it may be beneficial to explore the circularly polarized emission of the complexes **2c′** and **3c′**, and other parent compounds, following chiral resolution.

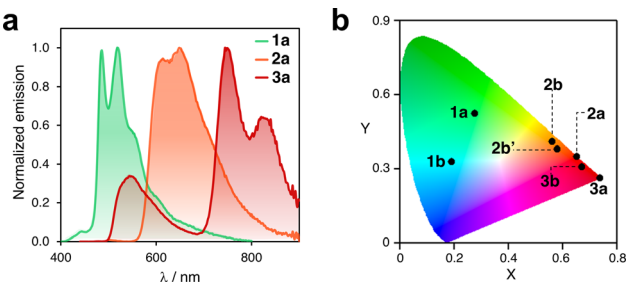

Fig. 5 (a) Emission spectra of complexes **1a**, **2a**, and **3a** in DCM at 25 °C. (b) CIE plot of selected Pt^{II} and Pt^{IV} cyclometalated complexes containing ligands **1**, **2** and **3**. Data corresponding to DCM solutions recorded at 25 °C.

Conclusions

In summary, our exploration of cyclometalated platinum complexes bearing compact, π-extended ligands has led to significant findings. The hindered rotation around the aryl–pyridine bond led to the discovery of unique rotamers, which had a pivotal impact on both structural and reactivity aspects. In particular, selective oxidation yielded Pt^{IV} complexes with symmetric and asymmetric structures, providing valuable insights into their reactivity and isolation. Our synthesized complexes show promising photophysical properties, particularly in the near-infrared region, which makes them suitable for use in bioimaging and optical sensors. This study advances the understanding of Pt complexes with extended π-conjugation, providing opportunities for future research and applications.

Data availability

All experimental procedures, mechanistic investigations, characterisation data, NMR spectra and computational data can be found in the article or in the ESI.† Crystallographic data for

compounds analyzed by SCXRD have been deposited at the CCDC under deposition numbers CCDC Deposition Numbers: 2357023 (**2b′**), 2357024 (**2b**), 2357025 (**3b**), 2357026 (**2c**), 2357027 (**3c**), 2357028 (**3a**), 2357029 (**2a**), and 2357030 (**3b′**), and can be obtained from **https://www.ccdc.cam.ac.uk/**

Author contributions

M. J. MacLachlan, M. A. Soto and S. Ota designed the research. S. Ota conducted the experiments. S. Ota, M. A. Soto, B. O. Patrick and S. Kamal analyzed the data. F. Lelj performed DFT calculations. M. A. Soto and S. Ota co-write the manuscript. M. J. MacLachlan and M. A. Soto conducted general guidance, project directing, and manuscript revision.

Conflicts of interest

There are no conflicts to declare.

Acknowledgements

S. O. thanks Dr Maria Ezhova and Dr Zhicheng (Paul) Xia for help with NMR characterization. M. J. M thanks the Canada Research Chairs program and NSERC (Discovery Grant) for funding. We also acknowledge WPI Nano Life Science Institute (Kanazawa) for support.

Notes and references

1 G. van Koten, *Pure Appl. Chem.*, 1989, **61**, 1681–1694.
2 W. Paw and R. Eisenberg, *Inorg. Chem.*, 1997, **36**, 2287–2293.
3 P.-K. Chow, G. Cheng, G. S. M. Tong, W.-P. To, W.-L. Kwong, K.-H. Low, C.-C. Kwok, C. Ma and C.-M. Che, *Angew. Chem., Int. Ed.*, 2015, **54**, 2084–2089.
4 M. A. Soto, R. Kandel and M. J. MacLachlan, *Eur. J. Inorg. Chem.*, 2021, **2021**, 894–906.
5 A. Zucca, G. L. Petretto, S. Stoccoro, M. A. Cinellu, M. Manassero, C. Manassero and G. Minghetti, *Organometallics*, 2009, **28**, 2150–2159.
6 M. V. Nikolaeva and M. V. Puzyk, *Opt. Spectrosc.*, 2013, **114**, 247–250.
7 C. A. Craig, F. O. Garces, R. J. Watts, R. Palmans and A. J. Frank, *Coord. Chem. Rev.*, 1990, **97**, 193–208.
8 J.-Y. Cho, K. Y. Suponitsky, J. Li, T. V. Timofeeva, S. Barlow and S. R. Marder, *J. Organomet. Chem.*, 2005, **690**, 4090–4093.
9 D. Septiadi, A. Aliprandi, M. Mauro and L. De Cola, *RSC Adv.*, 2014, **4**, 25709–25718.
10 A. Colombo, F. Fiorini, D. Septiadi, C. Dragonetti, F. Nisic, A. Valore, D. Roberto, M. Mauro and L. De Cola, *Dalton Trans.*, 2015, **44**, 8478–8487.
11 X. Wang, X. Wang and Z. Guo, *Acc. Chem. Res.*, 2015, **48**, 2622–2631.
12 H. Xu, R. Chen, Q. Sun, W. Lai, Q. Su, W. Huang and X. Liu, *Chem. Soc. Rev.*, 2014, **43**, 3259–3302.
13 T. Fleetham, G. Li and J. Li, *Adv. Mater.*, 2017, **29**, 1601861.
14 M. Kato, *Bull. Chem. Soc. Jpn.*, 2007, **80**, 287–294.
15 A. Aliprandi, D. Genovese, M. Mauro and L. De Cola, *Chem. Lett.*, 2015, **44**, 1152–1169.
16 G. Parrinello and J. K. Stille, *J. Am. Chem. Soc.*, 1987, **109**, 7122–7127.
17 I. E. Markó, S. Stérin, O. Buisine, G. Mignani, P. Branlard, B. Tinant and J.-P. Declercq, *Science*, 2002, **298**, 204–206.
18 D. S. Black, G. B. Deacon and G. L. Edwards, *Aust. J. Chem.*, 1994, **47**, 217–227.
19 L. Chassot, E. Mueller and A. Von Zelewsky, *Inorg. Chem.*, 1984, **23**, 4249–4253.
20 M. M. Mdleleni, J. S. Bridgewater, R. J. Watts and P. C. Ford, *Inorg. Chem.*, 1995, **34**, 2334–2342.
21 T. Yamaguchi, F. Yamazaki and T. Ito, *J. Am. Chem. Soc.*, 2001, **123**, 743–744.
22 C. P. Newman, K. Casey-Green, G. J. Clarkson, G. W. V. Cave, W. Errington and J. P. Rourke, *Dalton Trans.*, 2007, 3170–3182.
23 S. R. Whitfield and M. S. Sanford, *Organometallics*, 2008, **27**, 1683–1689.
24 J. Mamtora, S. H. Crosby, C. P. Newman, G. J. Clarkson and J. P. Rourke, *Organometallics*, 2008, **27**, 5559–5565.
25 D. M. Jenkins and S. Bernhard, *Inorg. Chem.*, 2010, **49**, 11297–11308.
26 F. Juliá, G. Aullón, D. Bautista and P. González-Herrero, *Chem.–Eur. J.*, 2014, **20**, 17346–17359.
27 F. Juliá, D. Bautista, J. M. Fernández-Hernández and P. González-Herrero, *Chem. Sci.*, 2014, **5**, 1875–1880.
28 F. Juliá, D. Bautista and P. González-Herrero, *Chem. Commun.*, 2016, **52**, 1657–1660.
29 F. Juliá and P. González-Herrero, *Dalton Trans.*, 2016, **45**, 10599–10608.
30 F. Juliá, M.-D. García-Legaz, D. Bautista and P. González-Herrero, *Inorg. Chem.*, 2016, **55**, 7647–7660.
31 D. A. K. Vezzu, J. C. Deaton, J. S. Jones, L. Bartolotti, C. F. Harris, A. P. Marchetti, M. Kondakova, R. D. Pike and S. Huo, *Inorg. Chem.*, 2010, **49**, 5107–5119.
32 H. Fukagawa, T. Shimizu, H. Hanashima, Y. Osada, M. Suzuki and H. Fujikake, *Adv. Mater.*, 2012, **24**, 5099–5103.
33 J. C. López-López, D. Bautista and P. González-Herrero, *Inorg. Chem.*, 2023, **62**, 14411–14421.
34 M. A. Soto and M. J. MacLachlan, *Chem. Sci.*, 2024, **15**, 431–441.
35 M. A. Soto, V. Carta, R. J. Andrews, M. T. Chaudhry and M. J. MacLachlan, *Angew. Chem., Int. Ed.*, 2020, **59**, 10348–10352.
36 M. A. Soto, V. Carta, M. T. Cano, R. J. Andrews, B. O. Patrick and M. J. MacLachlan, *Inorg. Chem.*, 2022, **61**, 2999–3006.
37 M. A. Soto, M. T. Chaudhry, G. K. Matharu, F. Lelj and M. J. MacLachlan, *Angew. Chem., Int. Ed.*, 2023, **62**, e202305525.
38 M. A. Soto, V. Carta, I. Suzana, B. O. Patrick, F. Lelj and M. J. MacLachlan, *Angew. Chem., Int. Ed.*, 2023, **62**, e202216029.
39 H. Yang, H. Li, L. Yue, X. Chen, D. Song, X. Yang, Y. Sun, G. Zhou and Z. Wu, *J. Mater. Chem. C*, 2021, **9**, 2334–2349.
40 M. Kondrashov, D. Provost and O. F. Wendt, *Dalton Trans.*, 2016, **45**, 525–531.

41 S. A. Denisov, Y. Cudré, P. Verwilst, G. Jonusauskas, M. Marín-Suárez, J. F. Fernández-Sánchez, E. Baranoff and N. D. McClenaghan, *Inorg. Chem.*, 2014, **53**, 2677–2682.
42 C.-Z. Luo, P. Gandeepan, J. Jayakumar, K. Parthasarathy, Y.-W. Chang and C.-H. Cheng, *Chem.–Eur. J.*, 2013, **19**, 14181–14186.
43 J. A. Fernández-Salas, S. Manzini, L. Piola, A. M. Z. Slawin and S. P. Nolan, *Chem. Commun.*, 2014, **50**, 6782–6784.
44 G. Zhang, G. Lv, C. Pan, J. Cheng and F. Chen, *Synlett*, 2011, **2011**, 2991–2994.
45 J. Jin, Q. Wen, P. Lu and Y. Wang, *Chem. Commun.*, 2012, **48**, 9933–9935.
46 R. Cerón-Camacho, S. Hernández, R. Le Lagadec and A. D. Ryabov, *Chem. Commun.*, 2011, **47**, 2823–2825.
47 I. Omae, *J. Organomet. Chem.*, 2017, **848**, 184–195.
48 M. Kondrashov, S. Raman and O. F. Wendt, *Chem. Commun.*, 2014, **51**, 911–913.
49 R. E. N. Njogu, P. Fodran, Y. Tian, L. W. Njenga, D. K. Kariuki, A. O. Yusuf, I. Scheblykin, O. F. Wendt and C.-J. Wallentin, *Synlett*, 2019, **30**, 792–798.
50 N. P. Tsvetkov, E. Gonzalez-Rodriguez, A. Hughes, G. dos Passos Gomes, F. D. White, F. Kuriakose and I. V. Alabugin, *Angew. Chem., Int. Ed.*, 2018, **57**, 3651–3655.
51 X. Wang, W.-G. Liu, L.-T. Liu, X.-D. Yang, S. Niu, C.-H. Tung, L.-Z. Wu and H. Cong, *Org. Lett.*, 2021, **23**, 5485–5490.
52 I. Allison, H. Lim, A. Shukla, V. Ahmad, M. Hasan, K. Deshmukh, R. Wawrzinek, S. K. M. McGregor, J. K. Clegg, V. V. Divya, C. Govind, C. H. Suresh, V. Karunakaran, K. N. N. Unni, A. Ajayaghosh, E. B. Namdas and S.-C. Lo, *ACS Appl. Electron. Mater.*, 2019, **1**, 1304–1313.
53 A. F. Rausch, L. Murphy, J. A. G. Williams and H. Yersin, *Inorg. Chem.*, 2012, **51**, 312–319.
54 J. Wu, B. Xu, Y. Xu, L. Yue, J. Chen, G. Xie and J. Zhao, *Inorg. Chem.*, 2023, **62**, 19142–19152.